Available online at www.sciencedirect.com

ScienceDirect

Ceramics International 40 (2014) 1489–1494

CERAMICS INTERNATIONAL

www.elsevier.com/locate/ceramint

Rapid synthesis and thermal catalytic performance of N-doped ZnO/Ag nanocomposites

Juan Lu[a], Jia Zhu[a], Zuoshan Wang[a,b,*], Jialei Cao[a], Xiufeng Zhou[a]

[a]College of Chemistry, Chemical Engineering and Materials Science, Soochow University, Soochow 215021, China
[b]State Key laboratory of Prevention and Control of Explosion Disasters, Beijing Institute of Technology, Beijing 100081, China

Received 30 January 2013; received in revised form 5 July 2013; accepted 5 July 2013
Available online 11 July 2013

Abstract

N-doped ZnO/Ag nanocomposites were rapidly synthesized by a deflagration method within tens of seconds, using urea as fuel and citric acid as vesicant. Characterization results showed that the samples were nanoparticles with an average size of about 15 nm. Most of Ag existed in the form of metallic Ag (0), and N was doped into the composite in the form of acceptor impurities. Compared with pure ZnO, the N-doped ZnO/Ag nanocomposites possessed a remarkably enhanced catalytic efficiency on the thermal decomposition of ammonium perchlorate. This is particularly true for the sample containing 4.0% Ag as it offered the best catalytic performance and reduced the final decomposition temperature of AP to 290 °C from 453 °C. The mechanism showed that the high decomposition rate of AP was due to N doping and Ag modification being able to transfer efficiently electrons from ClO_4^- to NH_4^+ in ammonium perchlorate.

Keywords: B. Nanocomposites; C. Chemical properties; D. ZnO; E. Thermal applications

1. Introduction

Wurtzite zinc oxide (ZnO) is a semiconductor material which has a wide band gap of 3.37 eV and a large excitation binding energy of 60 MeV at room temperature [1]. It has been widely utilized as luminescent materials, optoelectronic components and optical catalysts. Many methods have been used in order to improve its photo-catalytic performance, such as semiconductor combination [2], noble metal deposition [3–7], transition metal doping [8,9], non-metal doping [10–12] and double elements doping [13–15]. Previous reports have claimed that N doping [16–17] or Ag modification [3,18,19] would efficiently improve the photo-catalytic activity of ZnO. It is well acknowledged that the photo-catalytic mechanism consists in the increase of the separation of the electrons and holes in ZnO, which is very similar to the thermal catalytic mechanism of the decomposition of ammonium perchlorate (AP). Therefore, we summarize that the N doping and Ag modification may also improve the thermal catalytic activity of ZnO for the decomposition of AP.

In addition, to the best of our knowledge, there are only a few reports about the synthesis of ZnO modified with Ag and doped with N simultaneously. Zhenjiang Li et al. [20] reported the synthesis of N-doped ZnO/Ag nanocomposites by a two-step liquid deposition approach with the plasma nitriding technology, and the samples exhibited an excellent photo-catalytic activity. Other researchers obtained Ag–N dual-doped ZnO films by different methods, such as the sol–gel method [21], the spray pyrolysis technique [22] and the ion beam assisted deposition method [23].

In this study, N-doped ZnO/Ag nanocomposites were rapidly synthesized by a deflagration method, which is simple and efficient. The obtained nanoparticles have a small particle size, and exhibit an excellent thermal catalytic efficiency on the decomposition of AP.

2. Material and methods

2.1. Preparation of pure ZnO, N-doped ZnO and N-doped ZnO/Ag nanocomposites

Typically, 3.0 g of $Zn(CH_3COO)_2 \cdot 2H_2O$ (Sinopharm, 99.0%, China), 0.12 g of $AgNO_3$ (Sinopharm, 99.0%, China),

*Corresponding author at: No.199, Ren'ai Road, Soochow Industry Park, Soochow 215123, China. Tel./fax: +86 0512 85187680.
E-mail address: zuoshanwang@suda.edu.cn (Z. Wang).

0272-8842/$ - see front matter © 2013 Elsevier Ltd and Techna Group S.r.l. All rights reserved.
http://dx.doi.org/10.1016/j.ceramint.2013.07.033

3.0 g of urea (Sinopharm, 99.0%, China) and 0.6 g of citric acid (Sinopharm, 99.5%, China) were mixed together and ground into homogeneous slurry in a ball mill. Then the slurry was put into a preheated muffle furnace to experience a series of processes such as evaporation, condensation, foaming, combustion, etc. The whole reaction lasted tens of seconds, and finally the pink flocculent powders were collected for characterization. Different amounts of $AgNO_3$ was added to the system to obtain the samples containing different proportions of Ag, designated as N–Ag–*x*, where "*x*" stands for the mass ratio of $AgNO_3$:$Zn(CH_3COO)_2 \cdot 2H_2O$. N-doped ZnO was synthesized by a similar preparation without adding $AgNO_3$. As urea is used as fuel in this reaction, the obtained samples must contain N. Therefore, pure ZnO with a similar crystal structure and particle size was prepared for comparison according to the method reported by Hong et al. [24].

2.2. Thermal catalytic performance

The catalytic activity of N-doped ZnO/Ag nanocomposites on thermal decomposition of AP was tested by the following steps. Firstly, AP and N-doped ZnO/Ag samples were mixed together with a fixed mass ratio (97:3) and ground in some ethanol solution. After ethanol was evaporated, the samples were tested by a differential scanning calorimeter (DSC) experiments. The activity of the catalyst was measured according to the decomposition temperature of AP.

2.3. Instruments

The crystalline phase was determined using an X-ray diffraction (D/ Max-IIIC, Shimadzu) instrument with Cu Kα radiation ($\lambda = 0.15406$ nm). The analysis of the element state was done with X-ray photoelectron spectroscopy (XPS) (ESCALAB 250, Thermo). Transmission electron microscopic (TEM) and high-resolution transmission electron microscopic (HRTEM) images were obtained on a JEM-2100 microscope (JEOL) equipped with the selected-area electron diffraction (SAED). Thermal catalytic performance was tested by the DSC apparatus (US Company, PE Diamond type).

3. Results

3.1. XRD

Fig. 1(a) showed the XRD patterns of pure ZnO, N-doped ZnO and N-doped ZnO/Ag nanocomposites containing different Ag proportions. All samples exhibited a wurtzite structure, and the main diffraction data were consistent with the standard data about α-ZnO (JCPDS no. 5-664). It seems that N and Ag did not change the initial crystal structure of ZnO. However, an enlarged image shown in Fig. 1(b) obviously revealed that compared with pure ZnO, the diffraction peaks of other samples moved slightly towards the small degrees, implying N was doped into ZnO lattice, leading to the expander of the crystal lattice as the radius of N^{3-} ions is a little larger than that of O^{2-} ions.

Besides, when the proportion of $AgNO_3$ reached 1%, diffraction peaks assigned to metallic Ag (0) appeared and subsequently increase in the amount of $AgNO_3$ caused the peaks of Ag (0) to become more and more obvious. In comparison with Zn^{2+} ions, Ag^{+} ions have a much larger radius (0.072 nm and 0.122 nm respectively), and the X-ray

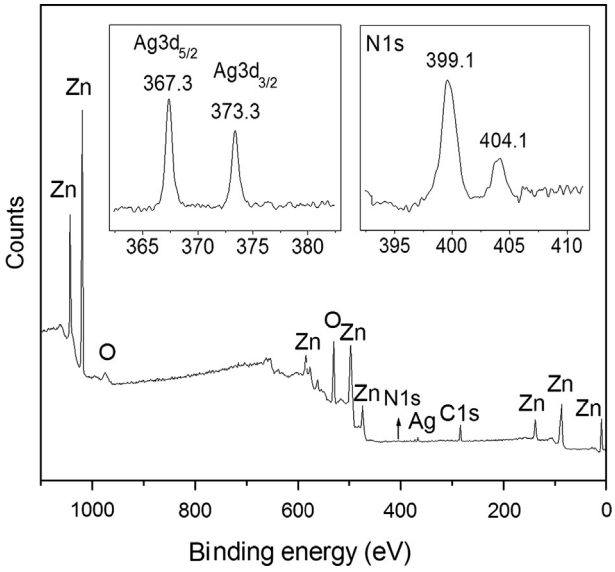

Fig. 2. XPS spectra of the sample N–Ag-4%.

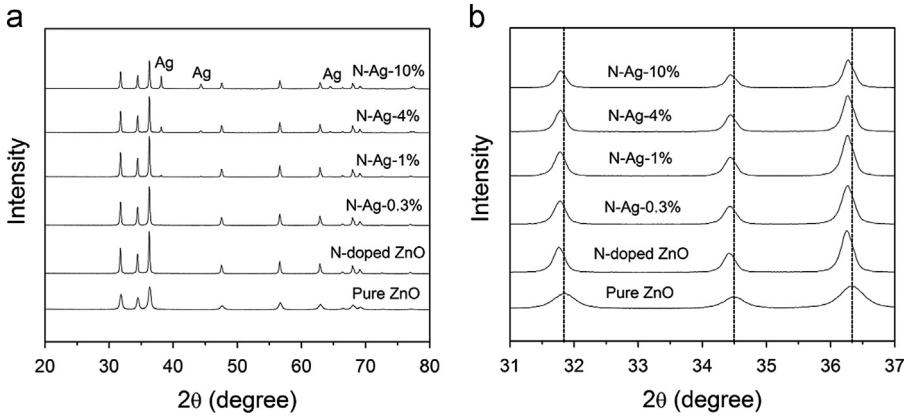

Fig. 1. (a) XRD patterns of the samples and (b) an enlarged image of (a).

peaks would visibly shift towards the small diffraction degree if Ag^+ ions were incorporated into the ZnO lattice [25]. However, this could not be observed in our experiment. In addition, there were no peaks belonging to any other materials, such as Ag_2O or AgO. Therefore, we can conclude that most of Ag existed in the form of metallic Ag (0).

3.2. XPS analysis

XPS analyses were performed to further study the existing states of N and Ag in our samples, and the typical result was shown in (Fig. 2). The insets displayed the high-resolution peaks of Ag3d and N1s regions. The peak located at 399.1 eV in the N1s XPS spectrum is ascribed to oxynitride ($ZnO_{1-x}N_x$) [26], and another weak peak located at 404.1 eV is related to nitrogen molecule at O sites [27]. No obvious signals indexed to free N or N radicles could be detected, implying the N existed in the form of acceptor impurities. The two peaks located at 367.3 eV and 373.3 eV are respectively attributed to $Ag3d_{5/2}$ and $Ag3d_{3/2}$. Compared with the bulk Ag ($Ag3d_{5/2}$ and $Ag3d_{5/2}$ are respectively 368.2 eV and 374.2 eV), the peaks of our sample shift obviously toward the lower binding

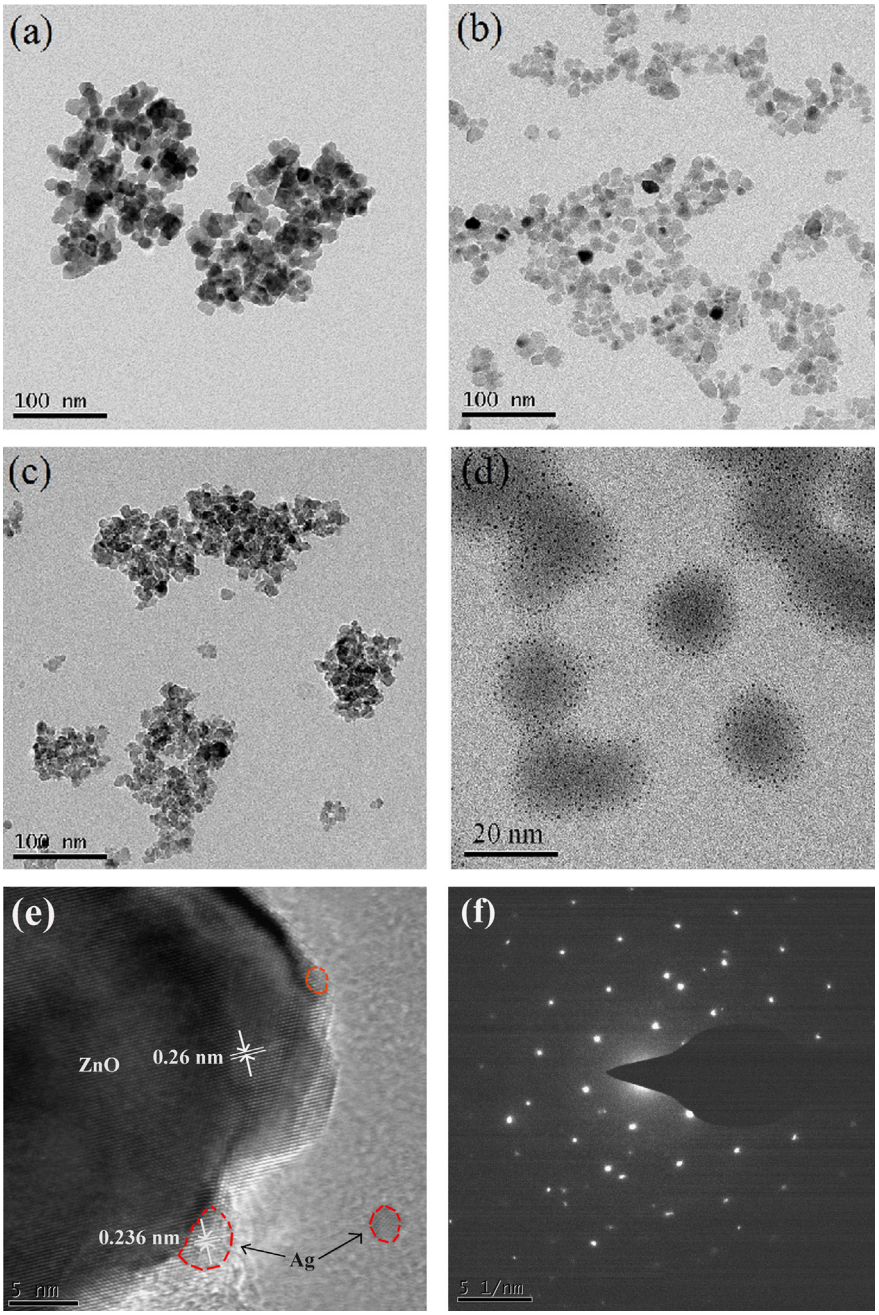

Fig. 3. TEM images of different samples: (a) pure ZnO; (b) N-doped ZnO; (c) and (d) N–Ag-4%; (e) and (f) HRTEM image and the corresponding SAED pattern of the sample N–Ag-4%, respectively.

energy, mainly due to the interaction between Ag and ZnO [25]. It was further confirmed that most of Ag existed in the form of metallic Ag (0) rather than Ag^+ ions.

3.3. TEM observations

Fig.3 showed the typical TEM images of pure ZnO, N-doped ZnO and the sample N–Ag-4%. It was found that all these samples were nanoparticles with an average size of about 15 nm. Besides, we can observe many Ag nanoparticles appearing as small dark dots in Fig.3(d), and it is another proof of the existence of metallic Ag (0) in the samples. Fig. 3(e) and (f) respectively showed the HRTEM images and the corresponding diffraction patterns of the sample N–Ag-4%. The spacing of two neighboring parallel fringes was 0.26 nm, which is assigned to the d spacing of the (002) planes of ZnO, and the spacing of 0.236 nm is ascribed to the Ag (111) planes, indicating that Ag (0) was contained in the sample. The HRTEM image and SAED pattern are in good agreement with their XRD pattern.

3.4. Thermal catalytic performance

DTA experiments demonstrated the catalytic effect of N-doped ZnO/Ag nanocomposites on the decomposition of AP and the results are showed in Fig. 4.

It is well acknowledged that there is one endothermic peak and two exothermic peaks in the DTA curve of pure AP (Fig. 4a). The endothermic peak around 249 °C denotes that the phase of AP undergoes a transition from rhombic to cubic. The first exothermic peak at about 325.7 °C belongs to the low-temperature decomposition of AP. During this process, AP partially decomposes to generate an intermediate product, and the remaining AP becomes a porous structure without any change in its chemical properties. The second exothermic peak at around 453 °C belongs to the high-temperature decomposition of AP, and it represents when AP is completely decomposed into volatile products.

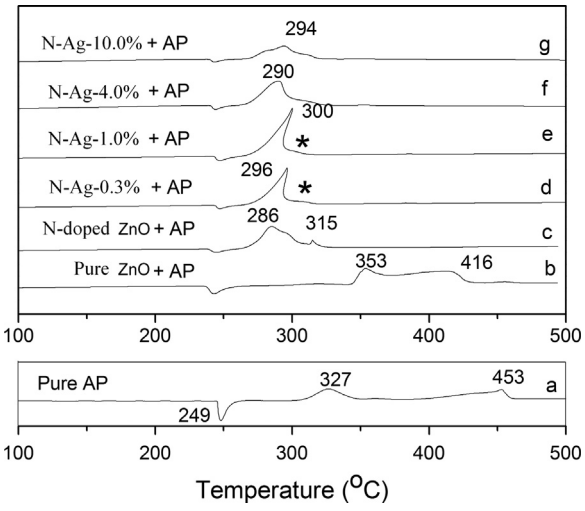

Fig. 4. DSC curves of AP thermal decomposition catalyzed by different samples.

When pure ZnO (Fig. 4b) was added into AP, the peak shape of the DTA curve became similar to the one of pure AP. However, the low-temperature decomposition peak moved backward, and the high-temperature decomposition peak moved forward, both remaining separate. It became even more conspicuous when the N-doped ZnO (Fig. 4c) was used as a catalyst. Dramatic changes were observed when N-doped ZnO/Ag nanocomposites (Fig. 4d–g) were used as the catalyst and it seemed as if the two exothermic peaks of AP had merged into one. The decomposition temperature had also been significantly lowered, which indicated that loading-Ag effectively improved the thermal catalytic activity of ZnO. However, the peaks in Fig. 4d and e are noticeably oblique, chiefly because the low- and high- temperature decomposition peaks have not really merged into one. And in fact, the weak peaks were indeed found at the positions marked with a star. When Ag was introduced with a proportion of 4.0% and 10%, the two exothermic peaks of AP actually merged into one. Of all the samples, N–Ag-4% (Fig.4f) is the one that offered the best catalytic performance and lowered the final decomposition temperature of AP to its lowest value of 290 °C from 453 °C. However, further increasing Ag – up to 10% – (Fig.4g) caused the decomposition temperature of AP to rise again.

4. Discussion

4.1. Reaction process of the rapid synthesis of N-doped ZnO/Ag nanocomposites

In this study, we have successfully synthesized N-doped ZnO/Ag nanocomposites by a deflagration method within tens of seconds in a muffle furnace which was preheated to 700 °C. During this process, $Zn(CH_3COO)_2 \cdot 2H_2O$ and $AgNO_3$ respectively decomposes to form ZnO and metallic Ag, and that latter will be dispersed in/on ZnO particles. The NH_3 produced by the reaction of urea and citric acid became the source of dopant N. Furthermore, urea worked also as the fuel and vesicant, and citric acid was used as assistant of the vesicant. When the acidic system is heated up, a lot of gases, such as NH_3, NO_2, CO_2 and H_2O would fill the entire system. These gases acted as natural barriers effectively preventing the product from agglomerating, which is the chief reason why these samples have a small particle size. The detailed reaction process has been listed as follows:

$$Zn(CH_3COO)_2 \cdot 2H_2O \rightarrow ZnO + CO_2\uparrow + H_2O\uparrow \quad (1)$$

$$AgNO_3 \rightarrow Ag + NO_2\uparrow \quad (2)$$

$$CO(NH_2)_2 + \text{citric acid} \rightarrow NH_3\uparrow + CO_2\uparrow \quad (3)$$

$$NH_3 + ZnO + Ag \rightarrow \text{N-doped ZnO/Ag} \quad (4)$$

We expect this method to be successful in the preparation of other nanocomposites, such as N-doped ZnO/Ce and N-doped ZrO_2/Ag.

4.2. Catalytic mechanism

4.2.1. Mechanism

Jacobs et al. [28,29] consider that the step which can efficiently control the decomposition rate of AP is the transfer of electrons from ClO_4^- to NH_4^+. The process was described as

$$ClO_4^- \rightarrow O + ClO_3^- \rightarrow 1/2O_2 + ClO_3^- + e^- \quad (5)$$

The equation shows that a higher number of positive holes in the reaction system are conducive to a positive reaction.

As we all know the photo-catalytic mechanism of N-doped ZnO/Ag nanocomposites consists in the increase of the separation of the electrons and holes in ZnO, and the separated electrons and holes will react respectively with O_2 and H_2O to form oxygen radicals and hydroxyl radical species ($\bullet O_2^-$, $\bullet HO_2$ and $\bullet OH$) which are extremely strong oxidants for the decomposition of organic chemicals [3]. However, in thermal catalysis, the contributing materials are the positive holes which will effectively consume the electrons generated by the reduction of ClO_4^-, and this is conducive to the decomposition of AP. Although the contributing materials are not exactly the same, increase in the number of positive holes is always beneficial to both photo-catalytic and thermal catalytic activities of ZnO. Therefore, we imitate the photo-catalytic mechanism to draw a schematic diagram of the thermal catalytic mechanism, as shown in Fig.5, and based on this, the roles of ZnO, N doping and Ag modification respectively in the thermal catalysis were discussed in detail as follows.

4.2.2. The influence of ZnO

Transition metal oxide plays the role of a bridge in the electron transfer process. When ZnO is heated, the electrons in the valence band become excited and transfer to the conduction band. At a lower temperature, a part of the electrons in AP transfers to the conduction band of ZnO [30], which causes the number of electrons transferring from ClO_4^- to NH_4^+ reduced and finally results in an increase of the decomposition temperature. However, the electrons deposited in the conduction band of ZnO are conducive to the high-temperature decomposition of AP, which causes the decomposition temperature to decrease significantly. That is why the low-temperature decomposition peak moved backward and the high-temperature decomposition peak moved forward when ZnO was used as the catalyst.

4.2.3. The influence of N doping

N-doped nanocomposites exhibit p-type semiconductor characteristics and transition of an electron from valence band to conduction band will need less energy in N-doped nanocomposites [21]. Thus, during the high-temperature decomposition, the deposited electrons in the conduction band of ZnO with high energies would transfer to NH_4^+ more easily and make the temperature decrease greatly. In this case, the low-temperature decomposition and the high-temperature decomposition merged into one process with a large amount of heat release at a relative low temperature, implying that the N-doped ZnO has effective catalysis in decomposition of AP.

4.2.4. The influence of Ag

As an excellent conductor, metallic Ag has a smaller work function (4.26 eV) than the one of ZnO (5.2 eV), which entails that, when they get in contact, the electrons will migrate from silver to the conduction band of ZnO in order to achieve the Fermi lever equilibration [3]. The process can be expressed as

$$Ag \rightarrow Ag^+ + e^- \quad (6)$$

$$Ag^+ + e^- \rightarrow Ag \quad (7)$$

When ZnO is heated up to a high temperature, electrons in the valence band will become excited and transfer to the conduction band with a simultaneous generation of the same amount of holes left behind. The deflexed energy band in the space charge region facilitates the rapid transfer of the as-excited electrons from ZnO to Ag nanoparticles, and monovalent Ag is reduced to zero-valent Ag (Eq. 7). Consequently, more and more positive holes are left in the VB of ZnO, which is conducive to the decomposition of AP (Eq. 5).

In addition, loading Ag with an optimal proportion was conducive to the decomposition of AP. However, when the proportion of Ag is above the optimal value, the silver particles loading on the surface of ZnO will become the recombination center of electrons and holes because of the electrostatic attraction between negatively charged silver and positively charged holes [31]. This will lead to a decrease in the number of the positive holes, which is not conducive to the decomposition of AP. That is why the decomposition temperature decreased first and increased later, when increasing the content of Ag, as N-doped ZnO/Ag composites were used as the catalyst.

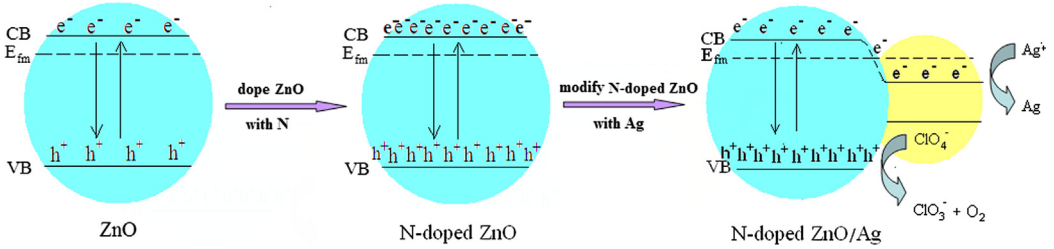

Fig. 5. An energetic diagram of ZnO-based catalysts.

5. Conclusions

N-doped ZnO/Ag nanocomposites were rapidly synthesized by a deflagration method. Characterization results showed that the obtained samples were nanoparticles with an average size of about 15 nm. Most of Ag existed in the form of metallic Ag (0), and N was doped into ZnO lattice in the form of acceptor impurities. DSC tests showed that compared with pure ZnO, N-doped ZnO and N-doped ZnO/Ag nanocomposites possessed a remarkably enhanced catalytic efficiency for the decomposition of AP. Among all the samples, the composite containing 4.0% Ag and N had the best catalytic performance, which reduced the decomposition temperature of AP to its lowest value of 290 °C from 453 °C. The mechanism showed that N doping and Ag modification would transfer the electrons from ClO_4^- to NH_4^+ efficiently in AP, which is the chief factor responsible for the decrease of the decomposition temperature of AP.

Acknowledgments

The authors are grateful for the financial support provided by the Explosion Science and Technology Key Laboratory Foundation of China (KFJJ09-7) and a Project funded by the Priority Academic Program Development of Jiangsu Higher Education Institutions.

References

[1] C.Y. Zuo, J. Wen, S.L. Zhu, C. Zhong, The effect of C–Al (Ga) codoping on p-type tendency in zinc oxide by first-principles, Optical Materials 32 (2010) 595–598.
[2] Y.C. Liao, C.S. Xie, Y. Liu, H. Chen, H.Y. Li, J. Wu, Comparison on photocatalytic degradation of gaseous formaldehyde by TiO_2, ZnO and their composite, Ceramics International 38 (2012) 4437–4444.
[3] D.D. Lin, H. Wu, R. Zhang, W. Pan, Enhanced photocatalysis of electrospun Ag–ZnO heterostructured nanofibers, Chemistry of Materials 21 (2009) 3479–3484.
[4] X.T. Yin, W.X. Que, D. Fei, F.Y. Shen, Q.S. Guo, Ag nanoparticle/ZnO nanorods nanocomposites derived by a seed-mediated method and their photocatalytic properties, Journal of Alloys and Compounds 524 (2012) 13–21.
[5] Y.H. Xiao, L.Z. Lu, A.Q. Zhang, Y.H. Zhang, L. Sun, L. Huo, et al., Highly enhanced acetone esnsing performances of porous and single crystalline ZnO nanosheets:high percentage of exposed (100) facets working together with surface modification with Pd nanoparticles, Applied Materials and Interfaces 4 (2012) 3797–3804.
[6] Y. Zhang, Q. Xiang, J.Q. Xu, P.C. Xu, Q.Y. Pan, F. Li, Self-assemblies of Pd nanoparticles on the surfaces of single crystal ZnO nanowires for chemical sensors with enhanced performances, Journal of Materials Chemistry 19 (2009) 4701–4706.
[7] F. Li, Y. Ding, P.X. Gao, X.Q. Xin, Z.L. Wang, Single-crystal hexagonal disks and rings of ZnO: lower-temperature, large-scale synthesis and growth mechanism, Angewandte Chemie International Edition 43 (2004) 5238–5242.
[8] D.H. Kim, D.K. Choi, S.J. Kim, K.S. Lee, The effect of phase type on photocatalytic activity in transition metal doped TiO_2 nanoparticles, Catalysis Communications 9 (2008) 654–657.
[9] C. Karunakaran, A. Vijayabalan, G. Manikandan, Photocatalytic and bactericidal activities of hydrothermally synthesized nanocrystalline Cd-doped ZnO, Superlattices and Microstructures 51 (2012) 443–453.
[10] S.S. Shinde, C.H. Bhosale, K.Y. Rajpure, Photocatalytic degradation of toluene using sprayed N-doped ZnO thin films in aqueous suspension, Journal of Photochemistry and Photobiology B, 113, 2012, pp. 70–77.
[11] H.F. Zhang, Z. Tao, W.G. Xu, S.X. Lu, F. Yuan, First-principles study of dopants and defects in S-doped ZnO and its effect on photocatalytic activity, Computational Materials Science 58 (2012) 119–124.
[12] S.S. Shinde, C.H. Bhosale, K.Y. Rajpure, First-principles study of dopants and defects in S-doped ZnO and its effect on photocatalytic activity, Solid State Electronics 68 (2012) 22–26.
[13] K. Zhong, J. Xu, J. Su, Y.L. Chen, Upconversion luminescence from Er–N codoped of ZnO nanowires prepared by ion implantation method, Applied Surface Science 257 (2011) 3495–3498.
[14] W.J. Lee, S.J. Shin, D.R. Juag, J.M. Kim, C.W. Nahm, T. Moon, et al., Investigation of electronic and optical properties in Al − Ga codoped ZnO thin films, Current Applied Physics 12 (2012) 628–631.
[15] L.L. Wu, Z.G. Gao, E. Zhang, H. Gao, H. Li, X.T. Zhang, Synthesis and optical properties of N–In codoped ZnO nanobelts, Journal of Luminescence 130 (2010) 334–337.
[16] M. Mapa, C.S. Gopinath, Combustion synthesis of triangular and multifunctional $ZnO_{1-x}N_x$ ($x \leq 0.15$) materials, Chemistry of Materials 21 (2009) 351–359.
[17] D.M. Bagnall, Optically-pumped lasing of ZnO at room temperature, Applied Physics Letters 70 (1997) 2230–2232.
[18] C.X. Song, Y.S. Lin, D.B. Wang, Z.S. Hu, Facile synthesis of Ag/ZnO microstructures with enhanced photocatalytic activity, Materials Letters 64 (2010) 1595–1597.
[19] C.D. Gu, C. Cheng, H.Y. Huang, T.L. Wong, et al., Growth and photocatalytic activity of dendrite-like ZnO@Ag heterostructure nanocrystals, Crystal Growth and Design 9 (2009) 3278–3285.
[20] Z.J. Li, S.Y. Sun, X. Xu, B. Zheng, A.L. Meng, Photocatalytic activity and DFT calculations on electronic structure of N-doped ZnO/Ag nanocomposites, Catalysis Communications 12 (2011) 890–894.
[21] L. Duan, W.X. Zhang, X.C. Yu, Z.Q. Jiang, L.J. Luan, Y.N. Chen, et al., Annealing effects on properties of Ag–N dual-doped ZnO films, Applied Surface Science 258 (2012) 10064–10067.
[22] R. Swapna, M.C. Santhosh Kumar, Deposition of the low resistive Ag–N dual acceptor doped p-type ZnO thin films, Ceramics International 39 (2013) 1799–1806.
[23] Z. Yan, Y.P. Ma, P.R. Deng, Z.S. Yu, C. Liu, Z.T. Song, Ag–N doped ZnO film and its p–n junction fabricated by ion beam assisted deposition, Applied Surface Science 256 (2010) 2289–2292.
[24] R.Y. Hong, J.H. Li, L.L. Chen, Q.Q. Liu, H.Z. Li, Y. Zheng, et al., Syntheisis surface modification and photocatalytic property of ZnO nanoparticles, Powder Technology 189 (2009) 426–432.
[25] Y.Y. Tay, S. Li, C.Q. Sun, P. Chen, Size dependence of Zn 2p3/2 binding energy in nanocrystalline ZnO, Applied Physics Letters 88 (2006) 173118-1–3.
[26] N. Tabet, M. Faiz, A. Al-Oteibi, XPS study of nitrogen-implanted ZnO thin films obtained by DC-magnetron reactive plasma, Journal of Electron Spectroscopy 163 (2008) 15–18.
[27] J.Z. Wang, E. Elamurugu, V. Sallet, F. Jomard, A. Lusson, A.M. Botelho do Rego, et al., Effect of annealing on the properties of N-doped ZnO films deposited by RF magnetron sputtering, Applied Surface Science 254 (2008) 7178–7182.
[28] P.W.M. Jacobs, R.J. Acheson, High-temperature thermal decomposition of ammonium perchlorate, Journal of the Chemical Society 3 (1959) 837–846.
[29] R. Zhang, The Combustion and Catalysis of Solid Propellant, first ed., National University of Defense Technology Press, Changsha, 1987.
[30] Y.T. Li, Y.L. Wu, J.D. Hu, C.Y. Hu, Y.X. Li, Role and mechanism of rare earth oxides in decomposition of ammonium perchlorate, Chinese Journal of Rare Metals 31 (2007) 526–532.
[31] T. Tan, Y. Li, Y. Liu, B. Wang, X.M. Song, E. Li, H. Wang, H. Yan, Two-step preparation of Ag/tetrapod-like ZnO with photocatalytic activity by thermal evaporation and sputtering, Materials Chemistry and Physics 111 (2008) 305–308.